

# High-velocity collision of two black holes

Masaru Shibata, Hirotada Okawa, and Tetsuro Yamamoto

Graduate School of Arts and Sciences, University of Tokyo, Komaba, Meguro, Tokyo 153-8902, Japan

We study nonaxisymmetric collision of two black holes (BHs) with a high velocity  $v = |dx^i/dx^0| = 0.6\text{--}0.9c$  at infinity, where  $x^\mu$  denotes four-dimensional coordinates. We prepare two boosted BHs for the initial condition which is different from that computed by a simple moving-puncture approach. By extrapolation of the numerical results, we find that the impact parameter has to be smaller than  $\approx 2.5GM_0/c^2$  for formation of a BH in the collision for  $v \rightarrow c$ , where  $M_0c^2$  is the initial total ADM mass energy of the system. For the critical value of the impact parameter, 20–30% of mass energy and 60–70% of angular momentum are dissipated by gravitational radiation for  $v = 0.6\text{--}0.9c$ .

PACS numbers: 04.25.D-, 04.30.-w, 04.40.Dg

**I Introduction:** Clarifying formation process of mini black hole (BH) in higher-dimensional spacetimes has become an important issue since a possibility of BH formation in accelerators was pointed out. If our space is the 3-brane in large [1] or warped [2] extra dimensions, the Planck energy could be of  $O(\text{TeV})$  that may be accessible with planned particle accelerators. In the presence of the extra dimensions, a BH of very small mass may be produced in the accelerators and the evidence may be detected.

The possible phenomenology of a BH produced in accelerators was first discussed in [3] (see [4] for reviews). During the high-energy particle collision of sufficiently small impact parameter in a higher-dimensional spacetime, two particles will merge to form a distorted BH, and then, it settles down to a quasistationary state after emission of gravitational waves. The quasistationary BH will be soon evaporated by the Hawking radiation, implying that the quantum gravity effects will be important. The evaporation and quantum gravity effects [5] have been studied for yielding a plausible scenario (cf. [6] for related issues). By contrast, the analyses for BH formation and subsequent evolution by gravitational radiation have not yet been done in detail (but see [7]). These phases are described well in the context of general relativity [8], but due to its highly nonlinear nature, any approximation breaks down. Thus, numerical relativity simulation is the unique approach to study this phase.

In this paper, we present a new numerical-relativity study for high-velocity collision of two BHs in four dimensions. This is the first step for understanding the high-velocity collision of two BHs in higher-dimensional spacetimes. We perform simulations for two equal-mass BHs of no spin. A new approach is adopted for preparing the initial condition (see Sec. II). The velocity of each BH is chosen in the range,  $0.6\text{--}0.9c$  (where  $c$  is the speed of light), and the results are extrapolated to infer a result for  $v \rightarrow c$ . We determine the largest value of the impact parameter for formation of new BH and approximately determine the final mass and spin of the BH. In the following, we use the geometrical units in which  $c = G = 1$ .

**II Initial condition:** There are several methods for preparing initial condition for high-velocity collision of

two BHs. A popular method is the moving-puncture approach which has been adopted in a recent work for the head-on collision of two high-velocity BHs [7]. In the simple moving-puncture approach in which the three-spatial hypersurface is assumed to be initially conformally flat, the BHs are not in a stationary state in their own comoving frame and hence a large amount of spurious gravitational waves are included, as pointed out in [7]. To avoid this unsuitable property, in this paper, we use a *different* approach from the simple moving-puncture one: We superimpose two boosted BHs, as described below.

The line element of a nonrotating BH in the isotropic coordinates is written as

$$ds^2 = -\alpha_0^2 dt^2 + \psi_0^4(dx_0^2 + dy_0^2 + dz_0^2), \quad (1)$$

where

$$\alpha_0 = \left(1 - \frac{m_0}{2r_0}\right)\psi_0^{-1}, \quad \psi_0 = 1 + \frac{m_0}{2r_0}. \quad (2)$$

$r_0 = \sqrt{x_0^2 + y_0^2 + z_0^2}$  and  $m_0$  is the BH mass in the rest frame of the BH. By boosting the BH in the  $x$ -axis direction with the speed  $v$ , the line element becomes

$$ds^2 = -\Gamma^2(\alpha_0^2 - \psi_0^4 v^2)dt^2 + 2\Gamma^2 v(\alpha_0^2 - \psi_0^4)dtdx + \psi_0^4(B_0^2 dx^2 + dy^2 + dz^2), \quad (3)$$

where the new coordinates  $x^\mu$  are related to the original one by the Lorentz transformation as  $t = \Gamma(t_0 + vx_0)$ ,  $x = \Gamma(x_0 + vt_0)$ ,  $y = y_0$ , and  $z = z_0$ .  $\Gamma$  is the Lorentz factor,  $\Gamma = 1/\sqrt{1-v^2}$ , and

$$B_0^2 = \Gamma^2(1 - v^2\alpha_0^2\psi_0^{-4}). \quad (4)$$

Note that at  $t = 0$ ,  $r_0 = \sqrt{\Gamma^2 x^2 + y^2 + z^2}$ .

Because the exact solution of a boosted BH is described by Eq. (3), in the following, we consider initial data for which the spatial metric has the form

$$dl^2 = \psi^4(B^2 dx^2 + dy^2 + dz^2). \quad (5)$$

Before going ahead, we summarize the lapse function ( $\alpha$ ), nonzero-component of the shift vector ( $\beta^i$ ), and non-zero

components of extrinsic curvature ( $K_{ij}$ ) of the boosted BH at  $t = 0$ :

$$\alpha = \alpha_0 B_0^{-1}, \quad \beta^x = \frac{\alpha_0^2 - \psi_0^4}{\psi_0^4 - \alpha_0^2 v^2} v, \quad (6)$$

$$K_{xx} = \frac{\Gamma^2 B_0 x v}{r_0} \left[ 2\alpha_0' - \frac{\alpha_0}{2} [\ln(\psi_0^4 - \alpha_0^2 v^2)]' \right], \quad (7)$$

$$K_{yy} = K_{zz} = \frac{2\Gamma^2 x v \alpha_0 \psi_0'}{\psi_0 B_0 r_0}, \quad (8)$$

$$K_{xy} = \frac{B_0 v y}{r_0} \left[ \alpha_0' - \frac{\alpha_0}{2} [\ln(\psi_0^4 - \alpha_0^2 v^2)]' \right], \quad (9)$$

$$K_{xz} = \frac{B_0 v z}{r_0} \left[ \alpha_0' - \frac{\alpha_0}{2} [\ln(\psi_0^4 - \alpha_0^2 v^2)]' \right]. \quad (10)$$

The dash (') denotes the ordinary derivative with respect to  $r_0$  (e.g.,  $\alpha_0' = d\alpha_0/dr_0$ ), and  $K_{ij}$  is derived from

$$K_{ij} = \frac{1}{2\alpha} \left( D_i \beta_j + D_j \beta_i - \partial_t \gamma_{ij} \right). \quad (11)$$

$D_i$  denotes the covariant derivative with respect to three metric,  $\gamma_{ij}$ , and we use the relation  $\partial_t \gamma_{ij} = -\Gamma v \partial_{x_0} \gamma_{ij}$ .

Now, we describe initial data for two BHs. Although we adopt initial condition which *approximately* satisfies constraint equations in general relativity in this paper, a general framework is first summarized.

We write the conformal factor as

$$\psi = \psi_{\text{main}} + \phi, \quad (12)$$

$$\psi_{\text{main}} \equiv 1 + \frac{m_1}{2r_1} + \frac{m_2}{2r_2}, \quad (13)$$

where  $m_a$  denotes mass parameter of each BH,  $r_a = \sqrt{\Gamma^2(x - x_a)^2 + (y - y_a)^2 + z^2}$ , and  $(x_a, y_a, 0)$  denotes the location of each BH at  $t = 0$ . Namely, we express each BH by a moving-puncture framework in a modified form, in which  $r_a \neq \sqrt{(x - x_a)^2 + (y - y_a)^2 + z^2}$ .  $\phi$  is a correction term which should be determined by solving the Hamiltonian constraint.

This paper focuses on the equal-mass case in which  $m_1 = m_2 = m_0$ ,  $x_2 = -x_1 = x_0$  ( $\geq 0$ ),  $y_2 = -y_1 = b/2$  ( $> 0$ ). Two BHs are assumed to have the same absolute velocity but move in the opposite directions each other; i.e.,  $v_1 = -v_2 = v$  ( $> 0$ ). Here,  $b$  denotes the impact parameter. The total mass energy  $M_0$  and angular momentum  $J$  of the system are

$$M_0 = 2m_0\Gamma \quad \text{and} \quad J = m_0\Gamma v b, \quad (14)$$

and the nondimensional spin parameter of the system is

$$\frac{J}{M_0^2} = \frac{bv}{4m_0\Gamma}. \quad (15)$$

It is natural to expect that a new BH is formed after the collision whenever  $J/M_0^2 < 1$ , i.e.,  $b < 4m_0\Gamma/v$ .

Taking into account that the line element of a boosted BH is written by Eq. (3), we write  $B^2$  as

$$B^2 = \Gamma^2 \left[ 1 - v^2 \left( 1 - \frac{m_1}{2r_1} - \frac{m_2}{2r_2} \right)^2 \psi_{\text{main}}^{-6} \right]. \quad (16)$$

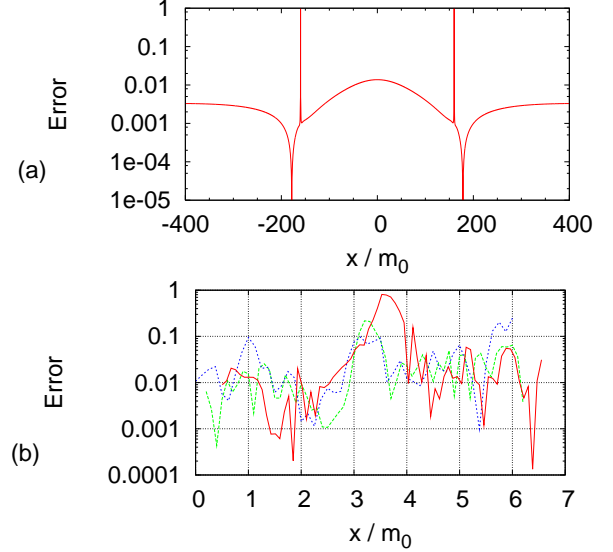


FIG. 1: (a) Violation of the Hamiltonian constraint along  $x$  axis for  $x_0 = 160m_0$ ,  $b = 0$ , and  $v = 0.9$ . The violation is defined by  $|H|/(|H_1| + |H_2| + |H_3|)$  where  $H_1 = \tilde{D}_i \tilde{D}^i \psi$ ,  $H_2 = -\tilde{R}\psi/8$ ,  $H_3 = [K_{ij}K^{ij} - (K^k_k)^2]\psi^5/8$ , and  $H = H_1 + H_2 + H_3$  should be zero if the Hamiltonian constraint is satisfied.  $\tilde{D}_i$  and  $\tilde{R}$  are the covariant derivative and Ricci scalar with respect to the conformal three metric  $\tilde{\gamma}_{ij} = \psi^{-4}\gamma_{ij}$ . (b) The same as (a) but for numerical results near one of BHs just before collision for  $x_0 = 160m_0$ ,  $bv/(m_0\Gamma) = 5.088$ , and  $v = 0.8$  in the simulations of different grid resolution,  $h/m_0 = 0.0625$  (dotted curve; at  $t = 256m_0$ ),  $0.050$  (dashed curve; at  $t = 256m_0$ ), and  $0.042$  (solid curve; at  $t = 258m_0$ ). BH is located for  $3 \lesssim x/m_0 \lesssim 4$ . Note that convergence is not seen because the degree of the constraint violation seems to be primarily determined by the initial condition.

For the extrinsic curvature, we basically superimpose two parts as

$$K_{ij} = K_{1ij} + K_{2ij} + \delta K_{ij}, \quad (17)$$

where  $K_{aij}$  ( $a = 1, 2$ ) are defined from Eqs. (7)–(10) by replacing  $r_0$  to  $r_a$  ( $a = 1, 2$ ).  $\delta K_{ij}$  is a correction term which should be determined by solving the momentum constraint.

In this paper, we adopt an approximate initial condition of  $\phi = 0$  and  $\delta K_{ij} = 0$ . The adopted initial data does not satisfy the constraint equations of general relativity for finite values of  $x_a$  and  $y_a$  or for nonzero value of  $v$ . However, for the case that  $R_a \equiv (x_a^2 + y_a^2)^{1/2}/m_0 \gg 1$ , the violation of the constraints is tiny because the magnitude of the violation is proportional to  $m_0/R_a$ . In the present work, we choose  $R_a/m_0 \gtrsim 100$  (typically 160) for the initial condition. In such case, the violation of the constraints is  $\sim m_0/R_a = O(0.01)$  for most of region (see Fig. 1), and thus, the initial condition approximately satisfies the constraints. The exception occurs around the puncture for which the violation is large, but the worst region is hidden inside apparent horizon and hence does not play a bad role. The constraint viola-

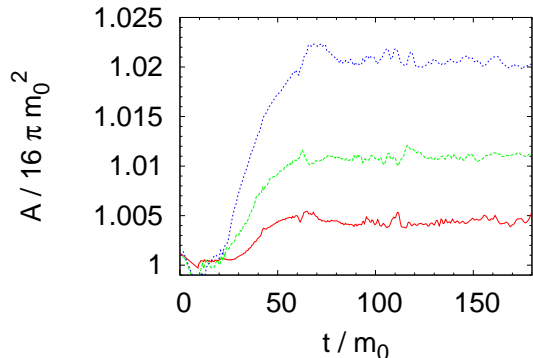


FIG. 2: Area of apparent horizon as a function of time before collision for  $v = 0.9$  and  $bv/(m_0\Gamma) = 4.708$  with different grid resolution,  $h/m_0 = 0.0625$  (dotted curve), 0.050 (dashed curve), and 0.042 (solid curve).

tion does not disappear during the evolution, but the magnitude of the violation remains roughly in the same small level at least before collision of two BHs (see Fig. 1(b)). In this method, the BHs are approximately in a stationary state in their own comoving frame and hence a large amount of spurious gravitational waves are not included, in contrast to the initial data prepared by the simple moving-puncture approach.

With this initial data, apparent horizons are located approximately for  $r_a = m_0/2$  at  $t = 0$ . The area of each horizon is  $\approx 16\pi m_0^2$  within the error of  $O(10^{-3})$  for  $x_a \gtrsim 100m_0$  (thus the bare mass of the BHs would be  $\approx m_0$ , and hence, a fraction of kinetic energy in the total mass of the system is  $1 - \Gamma^{-1}$ ). Furthermore, the area of the apparent horizon remains approximately  $16\pi m_0^2$  during evolution before collision (cf. Fig. 2). Therefore, it is reasonable to expect that numerical solution obtained by the simulation provides an approximate solution within an error of  $\sim 1\%$ . In the future work, we will perform simulations using improved initial data which satisfies the constraints, obtained by computing correction terms,  $\phi$  and  $\delta K_{ij}$ , to strictly validate the present strategy.

**III Numerical results:** For numerical simulation, we use SACRA code recently developed by our group [9]. In SACRA, the Einstein equations are solved in a modified version of BSSN (Baumgarte-Shapiro-Shibata-Nakamura) formalism [10] with a fourth-order finite differencing scheme in space and time and with an adaptive mesh refinement algorithm (at refinement boundaries, second-order interpolation scheme is partly adopted and hence the convergence may reduce to be second order). The moving-puncture approach is adopted for following moving BHs [11]. Gravitational waves are computed by extracting the outgoing part of the Newman-Penrose quantity (the so-called  $\Psi_4$ ). Properties of the BHs such as mass and spin are determined by analyzing area and circumferential radii of apparent horizons. The details of our schemes, formulation, gauge conditions, and methods for the analysis are described in [9]. This reference

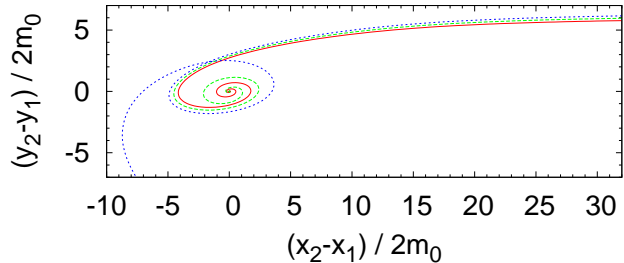


FIG. 3: Trajectories of relative position of moving punctures for  $v = 0.9$  and  $b/m_0 = 6.0, 6.2,$  and  $6.4$  (solid, dashed, and dotted curves). ( $bv/m_0\Gamma = 4.708, 4.865,$  and  $5.021.$ )

also shows that SACRA can successfully simulate merger of two equal-mass BHs. Because an adaptive mesh refinement algorithm is implemented, the moving BHs can be computed accurately by preparing a high-resolution domain appropriately around the BHs; in the present work, we prepare 10 refinement levels. Indeed, we performed test simulations in which a single high-velocity BH is boosted with  $v = 0.8$  and  $0.9$ , and found that our code can follow such high-velocity BH for more than  $500m_0$ ; e.g., we checked that the area of apparent horizon converges at approximately fourth order with improving grid resolution and the error is within  $\sim 0.1\%$  and  $1\%$  for  $v = 0.8$  and  $0.9$ , respectively, for the grid resolution with  $h = m_0/20$  (e.g., Fig. 2).

Numerical simulations are performed for  $v = 0.6, 0.7, 0.8,$  and  $0.9$  and  $x_0/m_0 = 160$  changing the impact parameter  $b$ . As expected from Eq. (15), two BHs should merge after collision for  $b < 4m_0\Gamma/v$ , and hence, the critical value of the impact parameter for the BH formation (hereafter  $b_{\text{crit}}$ ) should be close to  $4m_0\Gamma/v$ . For this reason, the value of  $b$  is chosen in the range,  $4 \lesssim bv/(m_0\Gamma) \lesssim 5.5$ , with the basic step size of  $b$  being  $0.1m_0$  (near  $b = b_{\text{crit}}$ , the step size of  $0.05m_0$  is partly used).

Numerical results depend only weakly on the initial separation for given values of  $v$  and  $b$ , and for a given grid resolution. Indeed, we performed detailed test simulations for  $v = 0.8$  and  $0.9$ , and  $x_0/m_0 = 80, 128,$  and  $160$ . If  $x_0/m_0$  is changed from 160 to 128, the value of  $b_{\text{crit}}$ , which is one of the most important outputs in this work, decreases only by  $\lesssim 0.05m_0$ , and from  $x_0/m_0 = 160$  to 80, by  $\lesssim 0.1m_0$ . Recall that the larger value of the initial separation results in the smaller initial constraint violation. Thus, the weak dependence of the numerical results on  $x_0$  indicates that the initial constraint violation only weakly affects the numerical results.

The numerical simulations are performed for different grid resolutions as  $h/m_0 = 0.075, 0.0625, 0.050,$  and  $0.042$ . The outer boundaries along each axis are located at  $L \approx 770m_0$  for all the grid resolution. The value of  $L/c$  is longer than the duration that the simulation is carried out, and hence, spurious effects from the outer

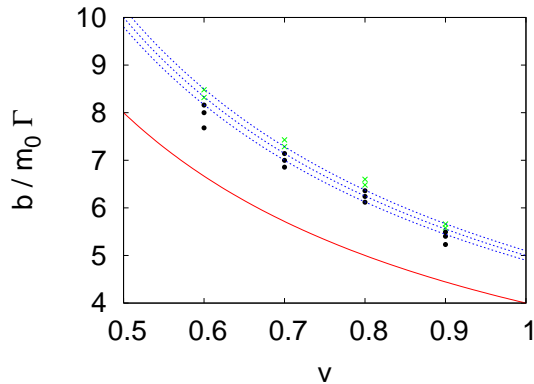


FIG. 4: Summary of the final outcomes after the collision of two BHs in the parameter space of  $(v, b)$ . The circles denote that a BH is formed after collision, whereas the crosses do not. The solid curve denotes  $b/(m_0\Gamma/v) = 4.0$ , and the dashed curves are 4.9, 5.0, and 5.1.

boundaries are excluded. We find that the value of  $b_{\text{crit}}$  depends only weakly on the grid resolution (it increases only by  $\sim 0.1m_0$  ( $\sim 1.5\%$ ) if we change  $h/m_0$  from 0.0625 to 0.042). The area of a BH formed after the merger, and total energy and angular momentum dissipated by gravitational waves ( $\Delta E$  and  $\Delta J$ ) depend more strongly on the grid resolution. However, our results indicate a convergence slightly better than second order with improving the grid resolution as long as  $h/m_0 \leq 0.0625$  and  $0.6 \leq v \leq 0.9$ , although the convergence becomes slow for  $v \gtrsim 0.9$ . This is natural because the coordinate radius of the apparent horizon in the  $x$ -axis direction for each BH is proportional to  $\Gamma^{-1}$ . Obviously, the better grid resolution is necessary for the ultra-high velocity collision  $v \rightarrow 1$ , but this is beyond scope of this paper.

Figure 3 plots trajectories of moving punctures for  $v = 0.9$ ,  $x_0 = 160m_0$ , and  $bv/(m_0\Gamma) = 4.708, 4.865,$  and  $5.021$ . Here, we plot relative position  $[(x_2 - x_1)/2m_0, (y_2 - y_1)/2m_0]$  on the orbital plane. For the first two impact parameters, the BH is formed after the collision, whereas for the other, each BH escapes from the center after scattering. For the small values of  $b$ , two BHs form a bound orbit when the orbital separation becomes small enough. For a sufficiently small value of  $b$ , such as  $bv/(m_0\Gamma) \lesssim 4.7$ , two BHs merge within one orbit. For a value of  $b$  close to  $b_{\text{crit}}$ , two BHs rotate around each other for more than one orbits before two BHs merge, as shown in Fig. 3. For  $b > b_{\text{crit}}$ , two BHs rotate around each other for small separation. However, they do not constitute a bound orbit because of the large centrifugal force, and eventually, each BH escapes from the center.

To summarize the outcomes after the collision, we generate Fig. 4 which shows a parameter space composed of  $(v, b)$ . We plot the circles for the case that two BHs merge after the collision, whereas the crosses are plotted when two BHs do not merge. The solid curve denotes  $b = 4m_0\Gamma/v$  for which the nondimensional spin parameter of the system is unity at  $t = 0$ . The three

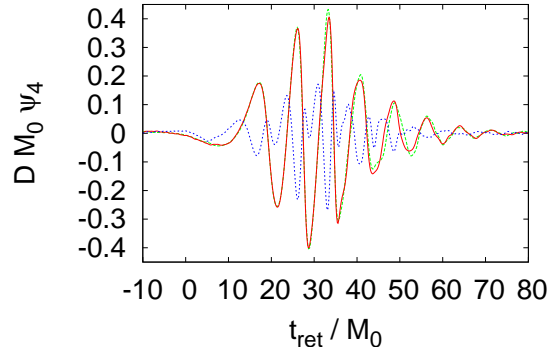


FIG. 5: Outgoing part of the Newman-Penrose quantity for  $v = 0.8$  and  $bv/(m_0\Gamma) = 5.088$ . The solid and dotted curves denote  $l = m = 2$  and  $l = m = 4$  modes for the best-resolved run, and the dashed curve denotes  $l = m = 2$  modes for the second-best run.  $t_{\text{ret}} = 0$  approximately corresponds to the time of the onset of merger.  $D$  denotes a distance between the source and observer.

dashed curves denote  $bv/m_0\Gamma = 4.9, 5.0,$  and  $5.1$ . Figure 4 clarifies that for  $b \lesssim b_{\text{crit}} \approx (5.0 \pm 0.1)m_0\Gamma/v$ , a BH is formed after the collision for the chosen velocity,  $0.6 \leq v \leq 0.9$ . Extrapolating the result for  $v \rightarrow 1$  under the assumption that the discovered relation holds even for  $v \rightarrow 1$ , the maximum impact parameter is determined to be  $(2.50 \pm 0.05)M_0$ .

Figure 5 plots outgoing part of the Newman-Penrose quantity for  $v = 0.8$  and  $bv/m_0\Gamma = 5.088$ .  $l = m = 2$  and  $l = m = 4$  modes are plotted for the best-resolved run with  $h = 0.042m_0$ . For  $l = m = 2$ , we also show the result for  $h = 0.05m_0$ , which agrees with the best-resolved result with a small error. Note that the waveforms are qualitatively similar irrespective of the value of  $v$  as far as  $b \approx b_{\text{crit}}$ , although the maximum amplitude steeply increases when  $b$  approaches  $b_{\text{crit}}$ . Figure 5 shows that gravitational waves are efficiently emitted after the onset of collision: When two BHs approach each other, amplitude of gravitational waves gradually increases. As the separation of two BHs becomes sufficiently small, they constitute a bound orbit and quasiperiodic gravitational waves are emitted. After substantial fraction of gravitational waves are emitted, two BHs merge to be a new BH, and then, ring-down gravitational waves associated with fundamental quasinormal modes are emitted for  $t_{\text{ret}} \gtrsim 40M_0$ . In this case, the formed BH is rapidly rotating with the spin parameter  $\approx 0.73 \pm 0.02$ , and hence, the damping time scale is longer than that for nonrotating BHs [12]. Because the orbital velocity is very large, higher-multipole components of gravitational waves are also enhanced significantly (cf. the waveform for  $l = m = 4$ ).

Total energy and angular momentum dissipated by gravitational waves are  $\approx 25 \pm 5\%$  and  $\approx 65 \pm 5\%$  of the initial energy and angular momentum, respectively, for  $b \lesssim b_{\text{crit}}$  and for  $v = 0.9$ . The totally emitted gravitational radiation for  $b \sim b_{\text{crit}}$  slightly decreases with

decreasing  $v$ , but still,  $\Delta E/M_0 \gtrsim 20\%$  and  $\Delta J/J \gtrsim 60\%$  for  $0.6 \leq v \leq 0.8$ .  $l = |m| = 4$  modes contribute to  $\Delta E$  and  $\Delta J$  by  $\approx 10\text{--}15\%$  and by  $\approx 15\text{--}20\%$ , respectively, for  $b \sim b_{\text{crit}}$ . It should be noted that in the limit  $b \rightarrow b_{\text{crit}}$ , total amount of gravitational radiation may be slightly larger than that presented here, because the lifetime of the formed binary orbit could be longer. We note that the results for the total amount of gravitational radiation are consistent with the mass and spin of the BH finally formed within an acceptable error for the best-resolved runs: The mass and angular momentum of the BHs estimated from apparent horizon are always smaller than those expected from gravitational radiation (i.e.,  $M_0 - \Delta E$  and  $J - \Delta J$ ) by  $\lesssim 0.05M_0$  and  $\lesssim 0.1J$ , respectively, for the best-resolved run. The error is larger for the larger value of  $v$ . The reason for this error is that energy and angular momentum are dissipated spuriously by numerical effects associated with finite grid resolution. However, our results show a behavior of convergence slightly better than second order with improving grid resolution.

**IV Discussion and summary:** We find that the largest value of the impact parameter for the BH formation after the collision is  $b_{\text{crit}} \approx (2.50 \pm 0.05)M_0/v$ . For such value of the impact parameter, the initial value of the spin parameter of the system is

$$\frac{J}{M_0^2} = 1.25 \pm 0.03. \quad (18)$$

For the BH formation, the spin parameter of the formed BH should be smaller than unity if the cosmic censorship holds [13]. This implies that a large fraction of

the angular momentum is dissipated by gravitational radiation during the collision. We estimate the total amount of the angular momentum and energy dissipated by gravitational radiation are  $\Delta J = (0.65 \pm 0.05)J$  and  $\Delta E = (0.25 \pm 0.05)M_0$ , respectively. The expected spin parameter of the formed BH is

$$\approx \frac{J - \Delta J}{(M_0 - \Delta E)^2} \approx (0.6 \pm 0.1) \frac{J}{M_0^2}. \quad (19)$$

Thus, even if the spin parameter of the system is initially 1.25, the resulting value at BH formation is smaller than unity. As this discussion clarifies, gravitational radiation increases the impact factor by  $\sim 25\%$ , and as a result, the cross section by  $\sim 50\%$ . It is also worth noting that the formed BH does not have an extremely large spin  $\sim 1$ , but approximately  $0.8 \pm 0.1$  even for  $b \lesssim b_{\text{crit}}$ .

In this work, we adopt initial data which satisfies the constraint equations only approximately. Although the violation is tiny (cf. Fig. 1), this error produces a small error in estimation of the critical cross section, and  $\Delta E$  and  $\Delta J$  of gravitational waves. To determine these quantities strictly, it is necessary to perform simulations using improved initial condition.

This work is a first step toward detailed understanding of high-velocity collision of two BHs in higher-dimensional spacetime. We plan to develop a numerical code for higher-dimensional spacetimes.

**Acknowledgments:** We thank T. Shiromizu and K. Maeda for helpful discussions and comments. This work was in part supported by Monbukagakusho Grant No. 19540263.

- 
- [1] N. Arkani-Hamed, S. Dimopoulos and G. R. Dvali, Phys. Lett. B **429**, 263 (1998); I. Antoniadis, N. Arkani-Hamed, S. Dimopoulos and G. R. Dvali, *ibid.* **436**, 257 (1998).  
 [2] L. Randall and R. Sundrum, Phys. Rev. Lett. **83**, 3370 (1999).  
 [3] T. Banks and W. Fischler, arXiv:hep-th/9906038; S. B. Giddings and S. Thomas, Phys. Rev. D **65**, 056010 (2002); S. Dimopoulos and G. Landsberg, Phys. Rev. Lett. **87**, 161602 (2001).  
 [4] M. Cavaglia, Int. J. Mod. Phys. A **18**, 1843 (2003); P. Kanti, Int. J. Mod. Phys. A **19**, 4899 (2004); S. Hossenfelder, arXiv:hep-ph/0412265.  
 [5] P. Kanti and J. March-Russell, Phys. Rev. D **66**, 024023 (2002); *ibid* **67**, 104019 (2003); D. Ida, K. Y. Oda and S. C. Park, Phys. Rev. D **67**, 064025 (2003); *ibid* **69**, 049901 (2004); *ibid* **71**, 124039 (2005).  
 [6] R. Emparan, G. T. Horowitz and R. C. Myers, Phys. Rev. Lett. **85**, 499 (2000); V. P. Frolov and D. Stojkovic, Phys. Rev. D **67**, 084004 (2003); *ibid* **68**, 064011 (2003); M. Cavaglia, Phys. Lett. B **569**, 7 (2003); V. P. Frolov and D. Stojkovic, Phys. Rev. Lett. **94**, 011603 (2005).  
 [7] U. Sperhake, V. Cardoso, F. Pretorius, E. Berti, and J. A. González, arXiv:0806.1738 (gr-qc).  
 [8] S. B. Giddings and V. S. Rychkov, Phys. Rev. D **70**, 104026 (2004).  
 [9] T. Yamamoto, M. Shibata, and K. Taniguchi, Phys. Rev. D **78**, 064054 (2008).  
 [10] M. Shibata and T. Nakamura, Phys. Rev. D **52**, 5428 (1995); T. W. Baumgarte and S. L. Shapiro, Phys. Rev. D **59**, 024007 (1998).  
 [11] M. Campanelli, C. O. Lousto, P. Marronetti, and Y. Zlochower, Phys. Rev. Lett. **96**, 111101 (2006); J. G. Baker, J. Centrella, D.-I. Choi, M. Koppitz, and J. van Meter, Phys. Rev. Lett. **96**, 111102 (2006).  
 [12] E. W. Leaver, Proc. R. Soc. Lond. A **402**, 285 (1985).  
 [13] E.g., R. M. Wald, *General Relativity*, (The University of Chicago Press, Chicago and London, 1984).